

Improving Corruption and Adversarial Robustness by Enhancing Weak Subnets

Yong Guo, David Stutz, Bernt Schiele
 Max Planck Institute for Informatics, Saarland Informatics Campus
 {yongguo, dstutz, schiele}@mpi-inf.mpg.de

Abstract

Deep neural networks have achieved great success in many computer vision tasks. However, deep networks have been shown to be very susceptible to corrupted or adversarial images, which often result in significant performance drops. In this paper, we observe that weak subnetwork (subnet) performance is correlated with a lack of robustness against corruptions and adversarial attacks. Based on that observation, we propose a novel robust training method which explicitly **identifies and enhances weak subnets (EWS) during training to improve robustness**. Specifically, we develop a search algorithm to find particularly weak subnets and propose to explicitly strengthen them via knowledge distillation from the full network. We show that our EWS greatly improves the robustness against corrupted images as well as the accuracy on clean data. Being complementary to many state-of-the-art data augmentation approaches, EWS consistently improves corruption robustness on top of many of these approaches. Moreover, EWS is also able to boost the adversarial robustness when combined with popular adversarial training methods.

1. Introduction

Since 2012, when AlexNet won the first place in the ImageNet competition [30], deep (convolutional) networks [32] have been producing state-of-the-art results in many challenging vision tasks [22, 33]. Recent work, however, highlights how brittle these models are when applied to slightly perturbed images [24, 59]: Natural or synthetic corruptions (such as noise, blur or image compression [24, 25]) as well as adversarial perturbations [14, 59], *i.e.*, imperceptibly perturbed images causing mis-classification, lead to significant accuracy drops. Regarding these issues, among an increasing body of work on developing robust models, the approaches based on heavy data augmentation are particularly effective against corruptions, including AutoAugment [10], AugMix [26] or DeepAugment [24]. By injecting adversarial examples into the training procedure, adversarial training [38] is used to “defend” against adversarial examples.

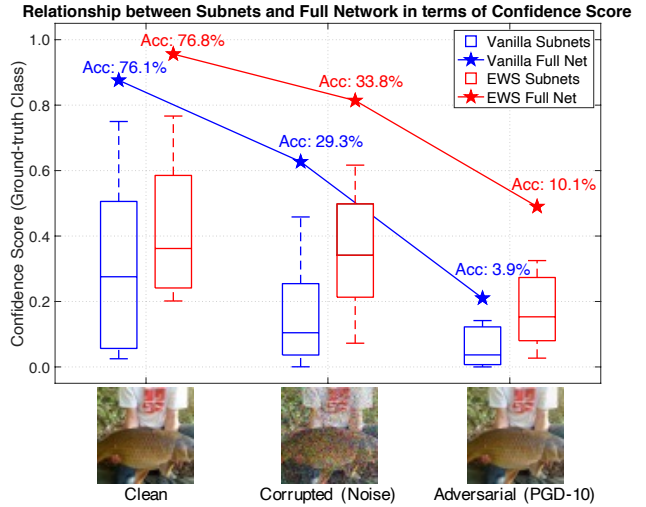


Figure 1. Performance of 1,000 randomly sampled subnets with 70% of paths/channels from a ResNet-50 on ImageNet. We report the **average confidence score** in the true class (y-axis). Box plots show the distribution of confidence scores across the subnets, stars show the overall performance of the full network. We compare a vanilla ResNet-50 (blue) with one trained while enhancing weak subnets (EWS, red). Clearly, confidence reduces significantly for the majority of subnets on corrupted images from ImageNet-C [25] or adversarial images generated using PGD [38]. Our approach (EWS) helps to reduce the impact of input perturbations significantly and improves overall performance.

While heavy augmentation and over-parameterized networks are often necessary for improving robustness [16, 43], it is well known that some well performing sub-networks (subnets) are responsible for the largest part of the obtained accuracy [12, 34, 52]. This leads us to the hypothesis that, on the other hand, those poorly performing (*i.e.*, *weak*) subnets are correlated with the lack of robustness of the full network. As shown in Figure 1, for a standard ResNet-50 [22] on ImageNet [48], we plot the confidence score in the true class (blue box plots) across randomly sampled subnets (see Section 3 for details). Clearly, the overwhelming majority of subnets perform very poorly on corrupted and adversarial images. This often goes along with significant performance drops of the full network (blue stars).

Contributions: In this paper, we address this issue through three key contributions. (1) We propose a novel robust training method which identifies and **enhances weak subnets (EWS)** to improve corruption and/or adversarial robustness of the full network. (2) To this end, we develop a search algorithm that obtains weak subnets by identifying weak paths/channels inside the full network. In particular, the search algorithm finds the subnets with the lowest accuracy. Given a weak subnet, its performance is further enhanced by distilling knowledge from the full network. (3) In experiments, we apply EWS on top of recent data augmentation schemes to improve corruption robustness on CIFAR-10-C and ImageNet-C [25]. Furthermore, adversarial robustness can be also improved significantly on top of popular adversarial training methods, including “vanilla” adversarial training (AT) [38], TRADES [69], and AWP [65]. The improvement is also reflected in the increased confidence scores in Figure 1 (red box plots and stars). We will make our code and pre-trained models publicly available.

2. Related Work

Despite their outstanding performance, many deep networks are not robust to various image transformations and corruptions, as demonstrated on CIFAR-10-C or ImageNet-C/R [24, 25]. Recent work explores re-calibrating batch normalization statistics [3, 42, 51], utilizing the frequency domain [49], vision transformers [40] or data augmentation [10, 13, 24, 26, 47] to improve corruption robustness. The latter is most prominent and ranges from simple Gaussian noise augmentation [47], over well-known schemes such as AutoAugment [10] to strategies specifically targeted towards corruption robustness such as AugMix [26] or DeepAugment [24]. These methods mix various basic augmentations or directly generate augmentations. Data augmentation can also be performed in an adversarial way [6, 50]. We emphasize that our work is complementary to these strategies in that EWS can further improve corruption robustness when combined with any of these techniques.

Besides random corruptions, deep networks are susceptible to adversarial images [14, 59]. While plenty of approaches for defending against adversarial examples have been proposed, see [1, 2, 4, 41, 45, 53, 66, 67], adversarial training is the current state-of-the-art in obtaining robust models [38]. Adversarial robustness has further been improved by various formulations of adversarial training [31, 64, 69] or using additional unlabeled examples [7, 17, 62], to name just a few examples. Adversarial training has also been applied to corruption robustness [28, 37] or to achieve robustness against multiple different attacks [39, 56, 60]. While [34, 52] find particularly robust subsets and [57, 65] employ adversarial training with weight perturbations, the poor robustness of subsets has not been addressed yet. However, we believe that subnets with poor robustness hamper the overall adversarial

robustness. Again, note that our EWS can be combined with any of these adversarial training methods.

Our approach is also inspired by recent work on neural architecture search (NAS) [5, 8, 21, 36, 71] and knowledge distillation (KD) [27, 70]. Recently, NAS has shown great success in designing effective neural architectures for various computer vision tasks [19, 35, 63]. Unlike them, we focus on improving the robustness of deep models and exploit NAS techniques to find weak subnets which may hamper the overall performance. Once we find these weak subnets we seek to further enhance them using a KD loss, similar to learning lightweight student models [15, 58].

3. EWS: Training by Enhancing Weak Subnets

In this paper, we seek to improve the robustness against image corruptions and adversarial attacks. Typically, corrupted images are obtained by introducing noise, blur, *etc.*, on standard benchmarks such as CIFAR-10-C and ImageNet-C [25]. Adversarial examples, in contrast, are maliciously and imperceptibly perturbed images with the intent of causing mis-classification. In Figure 1, we show that weak subnets of deep models perform particularly poorly on such corrupted or adversarial images, which directly translates to lower accuracies, as well. To address this, we propose a novel training method which improves robustness by *enhancing weak subnets (EWS)*: In Section 3.1, we first discuss the construction of subnets and the motivation for strengthening them. We then present an effective search algorithm to find weak subnets in Section 3.2. We further integrate the found weak subnets into our robust training method (see Figure 2, right) in Section 3.3. Here, we concentrate on corruption robustness, before extending EWS to adversarial training to improve adversarial robustness in Section 3.4. The training process of EWS is shown in Algorithm 1.

3.1. Subnet Construction and Motivation

We intend to investigate the robustness of deep networks from the perspective of smaller subnets. Given a full (convolutional, feedforward) network M , we construct a set of subnets $\alpha \in \Omega$ where Ω denotes the space of all the possible subnets of M . In this paper, we consider deep models that consist of a stack of basic blocks, *e.g.*, ResNet [22]. Without loss of generality, we allow each basic block i to have a specific number of paths n_i and each layer j in a block to have a specific number of channels c_j . For example, a basic residual block [22] contains $n_i = 2$ paths (including a residual path and a skip connection). As shown in Figure 3, we construct subnets by selecting a subset of paths and channels in each block and layer, respectively. Specifically, given a subnet width $\rho \in (0, 1)$, we select $\rho \cdot n_i$ paths in each block i and $\rho \cdot c_j$ channels for each layer j . In Figure 1, for example, $\rho = 0.7$ denotes selecting 70% paths/channels.

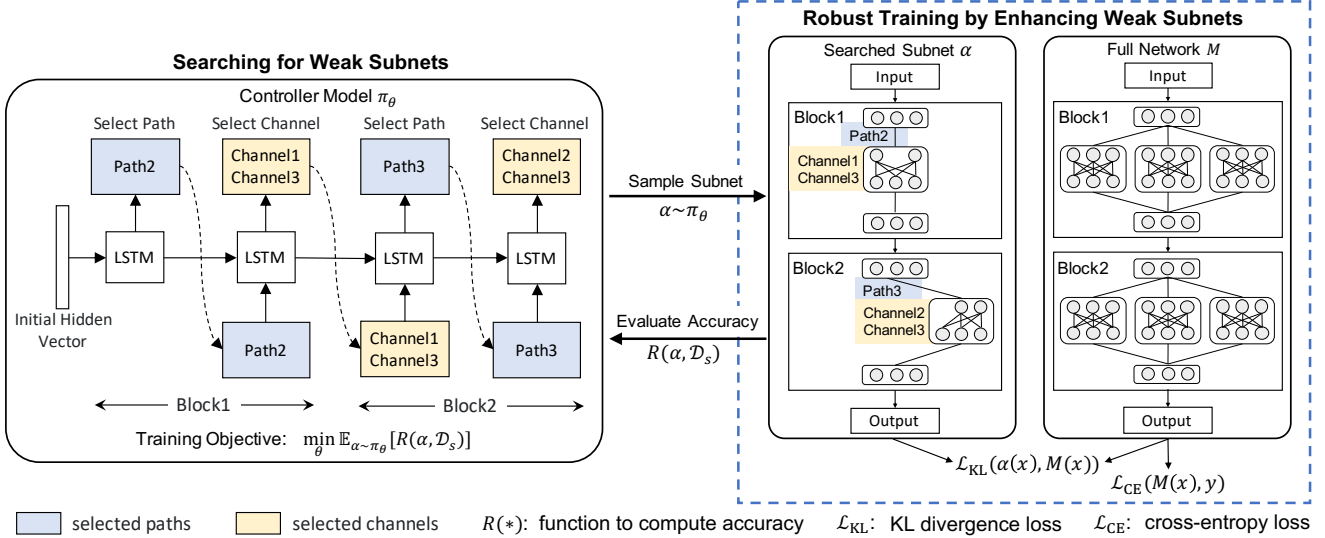


Figure 2. Overview of the proposed **enhancing weak subnets** (EWS) training method. During training, we alternatively perform subnet search based on a controller model (left) and train the full network with an additional distillation loss (right). As illustrated, the controller is implemented using an LSTM and trained using policy gradient every K epochs, while the full network can be any state-of-the-art (feedforward, convolutional) network such as ResNets [22]. This distillation loss enforces predictions of the full network and the found weak subnet to be similar. We refer to Algorithm 1 for a detailed description.

Motivation. Randomly sampling subnets allows to quantify their robustness on corrupted images and adversarial images: From Figure 1, despite the full network making the correct prediction with relatively high confidence score (blue stars), more than 50% of the subnets yield a confidence score lower than 0.3 (blue box plots) on clean examples (left). This means that there is a large number of weak, *i.e.*, poorly performing, subnets inside the full model. This is further emphasized on corrupted images (middle) where lower confidence scores of subnets also lead to poorer performance of the full network, *i.e.*, reducing accuracy from 76.1% to 29.3%. Finally, on adversarial images (right), *all* subnets obtain very low confidence scores and the full network is barely better, obtaining an accuracy of 3.9%. These observations motivate us to improve the overall robustness by explicitly finding and enhancing weak subnets. Motivated by this, the following sections present a novel robust training method which puts more focus on enhancing weak subnets (EWS) while training the full network. As shown in Figure 1, with the enhanced weak subnets (red box plots), we are able to greatly improve the robustness of the full network.

3.2. Searching for Weak Subnets

The proposed EWS has two core components: searching for weak subnets and strengthening their performance. Regarding the first component, given a search space Ω , we develop a new search algorithm to find weak subnets. As we are interested in finding particularly poorly performing ones, we evaluate a subnet α based on its classification accuracy $R(\alpha, \mathcal{D})$, considering some data set \mathcal{D} . As it is expensive

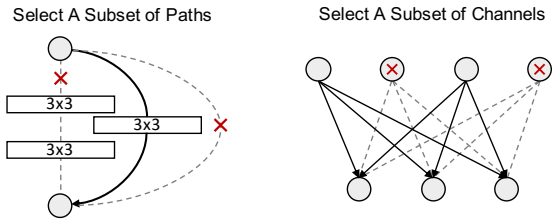


Figure 3. Illustration of constructing subnets by selecting a subset of paths and channels for each block and layer, respectively. Left: An example for a basic, ResNet-like block with multiple paths using skip connections. Right: For convolutional or fully connected layers, a subset of channels is selected. This approach is applied block-by-block, layer-by-layer using a fixed fraction of paths/channels to be selected. In particular, bold lines denote the selected paths/channels.

to compute the accuracy on the whole data set, we accelerate the search process, following [36, 44], using a data subset $\mathcal{D}_s \subset \mathcal{D}$ as proxy (see analysis on the subset size in supplementary). Furthermore, because there are many weak subnets which may contribute to the poor overall robustness, see Figure 1, we seek to find and enhance a set of weak subnets rather than an individual one. Thus, we learn a policy π_θ , parameterized by θ , and use it to generate candidate weak subnets, *i.e.*, $\alpha \sim \pi_\theta$. To learn the policy, we build a controller model to produce candidate subnets by minimizing the accuracy $R(\alpha, \mathcal{D}_s)$ in expectation. Formally, we solve the following optimization problem

$$\min_\theta \mathbb{E}_{\alpha \sim \pi_\theta} [R(\alpha, \mathcal{D}_s)]. \quad (1)$$

The controller’s parameters can be updated using policy gradient based on a mini-batch of sampled subnets (see the supplementary material for details). This step corresponds to Figure 2 (left) and is made explicit in Algorithm 1.

Architecture of the Controller Model. Since a whole network can be represented by a series of tokens [44], the subnet generation task can be viewed as a sequential decision making problem. Following [19, 20, 44], we build an LSTM-based [18] controller model to learn the policy π_θ . Specifically, the controller model takes an initial hidden state (kept constant during training) as input and sequentially selects paths/channels, starting from the first block/layer of the network. As shown in Figure 2 (left), for each block, we first select a subset of paths and then select a subset of channels for each layer in the selected paths. Please refer to the supplement materials for a more concrete example.

3.3. Improving Corruption Robustness with EWS

In the second step of EWS, based on the found weak subnets $\alpha \sim \pi_\theta$, we use a distillation loss to improve their performance and thereby aim to improve the overall robustness of the full network. This is motivated by the large gap of confidence score between the overall network (blue star) and the subnets (blue box plots) in Figure 1. Let x be the training example with its label y , which can be optionally augmented using data augmentation techniques [10, 24, 26]. Besides the standard cross-entropy (CE) loss, we introduce an additional Kullback-Leibler (KL) divergence loss between the full network output $M(x)$ and subnet prediction $\alpha(x)$. This can be thought of as distilling knowledge from the full network into the (weak) subnet. Thus, the loss function becomes

$$\mathcal{L}(x, y) = \mathcal{L}_{\text{CE}}(M(x), y) + \underbrace{\lambda \mathcal{L}_{\text{KL}}(\alpha(x), M(x))}_{\text{enhance weak subnet}}, \quad (2)$$

where λ is a trade-off coefficient determining the importance of enhancing weak subnets during training (see impact of λ in Section 5.1). While other losses for improving weak subnets are possible, *e.g.*, CE loss $\mathcal{L}_{\text{CE}}(\alpha(x), y)$, we found that the KL loss performs best in practice (see the supplementary for details). During training, we minimize this loss using SGD as highlighted in the second part of Algorithm 1.

It is worth noting that, once we update the model parameters, the previously learned controller (*i.e.*, the policy π_θ) is out-of-date. This is problematic as the sampled subnets $\alpha \sim \pi_\theta$ might not be particularly weak anymore after the update of model parameters. Thus, we train the model and controller in an alternating fashion as shown in Algorithm 1. However, training the controller model introduces additional computational cost. Regarding this issue, we find that it is not necessary to train the controller model in each epoch. In practice, we can obtain promising results when training the controller model every K epochs and greatly reduce the training cost (see impact of K in Section 5.1).

Algorithm 1 Training by **enhancing weak subnets (EWS)**:

We alternate between updating the controller model π_θ (every K epochs) and updating the model M . When training the model M , we sample a subnet $\alpha \sim \pi_\theta$ for each iteration and exploit a distillation loss to enhance it.

Require: Training data \mathcal{D} , batch size N , training data for search \mathcal{D}_s , batch size for search C , hyper-parameter λ , training interval K , number of epochs T

```

1: for  $i = 1, \dots, T$  do
2:   // Update the controller only every  $K$  epochs
3:   if  $i \bmod K = 0$  then
4:     for each iteration on  $\mathcal{D}_s$  do
5:       Sample a set of subnets  $\{\alpha_i\}_{i=1}^C$  from  $\pi_\theta$ 
6:       Compute subnet accuracy  $R(\alpha, \mathcal{D}_s)$ 
7:       Update  $\theta$  using policy gradient:
8:          $\theta \leftarrow \theta + \eta \frac{1}{C} \sum_{i=1}^C \nabla_\theta \log \pi_\theta(\alpha_i) R(\alpha_i)$ 
9:     end for
10:   end if
11:   // Train the full model while enhancing weak subnets
12:   for each iteration on  $\mathcal{D}$  do
13:     Sample batch of examples  $\{(x_i, y_i)\}_{i=1}^N$  from  $\mathcal{D}$ 
14:     Sample weak subnet  $\alpha \sim \pi_\theta$ 
15:     Update  $w$  using gradient descent:
16:        $w \leftarrow w - \eta \frac{1}{N} \sum_{i=1}^N (\nabla_w \mathcal{L}_{\text{CE}}(M(x_i), y_i) + \lambda \nabla_w \mathcal{L}_{\text{KL}}(\alpha(x_i), M(x_i)))$ 
15:   end for
16: end for

```

3.4. Improving Adversarial Robustness with EWS

As EWS only adds an additional KL-divergence loss between full network and subnet, it can easily be applied to adversarial training in order to improve robustness against adversarial examples. Again, since most subnets yield very low confidence on adversarial images, see Figure 1, we intend to improve the overall adversarial robustness by enhancing weak subnets. This also means that we seek to find adversarially vulnerable subnets, see Section 3.4.1, and then enhance them on adversarial images using state-of-the-art adversarial training protocols [38, 65, 69], see Section 3.4.2.

3.4.1 Searching for Vulnerable Subnets

Here, we seek to find weak/vulnerable subnets on adversarial images. Let ϕ be some loss function and ϵ be the bound for adversarial L_p perturbations. For example, $p = \infty$ is a common choice and ϕ could be the CE loss or a KL-divergence loss (following [38] or [69]). Given the clean images \mathcal{D}_s , we can generate adversarial images \mathcal{D}'_s by maximizing ϕ , *i.e.*, $\mathcal{D}'_s = \{x' | x' = \arg \max_{\|x-x'\|_p \leq \epsilon} \phi(x', y), x \in \mathcal{D}_s\}$. This is commonly achieved using projected gradient ascent (PGD), where the projection reduces to a simple clamping operation for $p = \infty$, see [38]. Thus, to find adversarially vul-

Method		Clean Error ↓	Corruption Error ↓
Standard	Vanilla	5.32 (-0.00)	26.46 (-0.00)
	Dropout	5.16 (-0.16)	26.17 (-0.29)
	EWS	4.12 (-1.20)	24.94 (-1.52)
AutoAugment [10]	Vanilla	4.05 (-0.00)	16.19 (-0.00)
	Dropout	3.91 (-0.14)	16.04 (-0.15)
	EWS	3.13 (-0.92)	14.31 (-1.88)
AugMix [26]	Vanilla	4.35 (-0.00)	13.57 (-0.00)
	Dropout	4.19 (-0.16)	13.44 (-0.13)
	EWS	3.56 (-0.79)	10.80 (-2.77)

Table 1. Clean and corrupted test error on CIFAR-10 and CIFAR-10-C, respectively. Our proposed EWS approach not only improves clean test error, but also reduces corrupted test error as highlighted in **bold**. This holds independent of the data augmentation scheme.

nerable subnets, we replace the (clean) accuracy $R(\alpha, \mathcal{D}_s)$ in Equation (1) with the adversarial accuracy $R(\alpha, \mathcal{D}'_s)$. Again, we follow Algorithm 1 and train the controller using policy gradient, only that the sampled subnets are evaluated on adversarial images instead of the clean ones.

3.4.2 Adversarial Training with EWS

With the found weak subnets, we again intend to enhance them with the goal to improve the overall adversarial robustness. Ideally, we seek to improve adversarial accuracy while preserving clean accuracy. Letting γ be a trade-off hyperparameter, we simultaneously optimize a loss on adversarial images $\mathcal{L}_a(x', y)$ and a loss on clean images $\mathcal{L}_c(x, y)$:

$$\min_w \mathbb{E}_{(x, y) \sim \mathcal{D}} [\mathcal{L}_a(x', y) + \gamma \mathcal{L}_c(x, y)]$$

where $x' = \arg \max_{\|x - x'\|_p \leq \epsilon} \phi(x', y)$. (3)

For both adversarial images x' and clean images x , we introduce an additional distillation-based KL divergence loss to enhance weak subnets. Formally, these losses become

$$\left\{ \begin{array}{l} \mathcal{L}_a(x', y) = \phi(x', y) + \underbrace{\lambda \mathcal{L}_{\text{KL}}(\alpha(x'), M(x'))}_{\text{enhance subnet on } x'} \\ \mathcal{L}_c(x, y) = \mathcal{L}_{\text{CE}}(M(x), y) + \underbrace{\lambda \mathcal{L}_{\text{KL}}(\alpha(x), M(x))}_{\text{enhance subnet on } x} \end{array} \right. \quad (4)$$

As before, λ determines the importance of weak subnet performance. This formulation subsumes popular, state-of-the-art adversarial training approaches, including [38] and [69]. In particular, the “vanilla” adversarial training (AT) is obtained using $\phi(x', y) = \mathcal{L}_{\text{CE}}(M(x'), y)$. AT commonly uses $\gamma = 0$, *i.e.*, training exclusively on adversarial examples (even though variants with $\gamma > 0$ have been studied as well [55]). Using $\phi(x', y) = \mathcal{L}_{\text{KL}}(M(x'), M(x))$, in contrast, usually with $\gamma = 1/6$, we obtain the TRADES [69] method. This illustrates that EWS is entirely complementary to many recently proposed adversarial training variants.

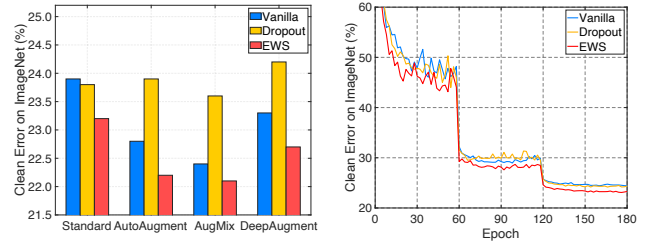


Figure 4. *Left:* Comparisons of clean top-1 test error on ImageNet. EWS consistently reduces error across diverse augmentation schemes. *Right:* Training curves in terms of top-1 test error on ImageNet using the standard data augmentation scheme. Clearly, the improvement of EWS can be observed throughout training.

4. Experiments

In the following, we exploit EWS to train models against corrupted and adversarial examples. First, in Section 4.1, we demonstrate that EWS boosts robustness against corrupted examples when applied on standard training as well as AutoAugment [10], AugMix [26] or DeepAugment [24]. In Section 4.2, we focus on improving adversarial robustness and apply EWS on top of vanilla adversarial training [38] as well as TRADES [69] and AWP [65]. Note that we provide ablation studies separately in Section 5.

4.1. Improving Corruption Robustness

We start by training EWS on standard benchmark datasets, *i.e.*, CIFAR-10 [29] and ImageNet [11], and testing not only on clean test examples but also on corrupted ones, namely CIFAR-10-C and ImageNet-C. These datasets contain examples with several common corruptions such as different noise, blur kinds, *etc.*. On CIFAR-10-C, we report standard test error on clean or corrupted examples. On ImageNet-C, in contrast, we report mean corruption error (mCE). We also consider ImageNet-P which evaluates prediction stability on videos using mean flip rate (mFR). For all the metrics, *lower is better*. In all experiments, by default, we set $K = 10$, $\lambda = 1$ and $\rho = 0.5$ for EWS in Algorithm 1.

4.1.1 Results on CIFAR-10

Experimental Setup. We compare different training methods based on a ResNet-50 with 400 training epochs. Besides the vanilla training method, we also compare our method with Dropout [54] which trains deep models by randomly dropping the internal connections. By default, we use random cropping and horizontal flipping as data augmentation. It is worth noting that data augmentation has shown great success in improving model robustness [10, 26]. Since our method is complementary to them, we further verify the proposed method based on several state-of-the-art augmentation methods, including AutoAugment [10] and AugMix [26].

Method	mCE ↓	Gauss.	Shot	Impul.	Defoc.	Glass	Motion	Zoom	Snow	Frost	Fog	Bright	Contra.	Elastic	Pixel	JPEG	
Standard	Vanilla	76.5 (-0.0)	80	82	83	75	89	78	80	78	75	66	57	71	85	77	77
	Dropout	76.5 (-0.0)	77	79	80	78	90	79	87	77	77	67	58	70	84	75	76
	EWS	75.1 (-1.4)	75	76	77	73	87	77	79	80	73	65	58	73	83	74	75
AutoAugment [10]	Vanilla	72.7 (-0.0)	69	68	72	77	83	80	81	79	75	64	56	70	88	57	71
	EWS	71.7 (-1.0)	67	68	71	78	82	78	79	78	73	64	55	69	86	56	72
AugMix [26]	Vanilla	68.4 (-0.0)	65	66	67	70	80	66	66	75	72	67	58	58	79	69	69
	EWS	67.5 (-0.9)	64	63	63	70	81	65	66	72	70	64	57	63	79	64	70
DeepAugment [24]	Vanilla	60.4 (-0.0)	49	50	47	59	73	65	76	64	60	58	51	61	76	48	67
	EWS	58.9 (-1.5)	48	47	45	58	71	63	73	65	59	56	50	60	74	47	66

Table 2. Mean corruption error (mCE) on ImageNet-C for vanilla data augmentation, AutoAugment, AugMix and DeepAugment. We consider all corruptions as well as individual ones. In all data augmentation settings, EWS reduces mCE significantly. Moreover, EWS improves over, *e.g.*, DeepAugment for almost all corruption types. We just report Dropout for the vanilla setting as it usually worsens mCE on top of AutoAugment, AugMix or DeepAugment.

Method	mFR ↓	Gaussian	Shot	Motion	Zoom	Snow	Bright	Translate	Rotate	Tilt	Scale	
Standard	Vanilla	58.0 (-0.0)	59	58	64	72	63	62	44	52	57	48
	Dropout	57.8 (-0.2)	62	59	65	52	48	58	63	57	44	72
	EWS	56.1 (-1.9)	62	55	62	49	45	52	64	52	42	71
AutoAugment [10]	Vanilla	51.7 (-0.0)	50	45	57	68	63	53	40	44	50	46
	EWS	50.4 (-1.3)	48	44	53	70	62	52	36	45	49	45
AugMix [26]	Vanilla	37.4 (-0.0)	46	41	30	47	38	46	25	32	35	33
	EWS	36.6 (-0.8)	45	39	31	42	33	43	39	35	27	32
DeepAugment [24]	Vanilla	32.1 (-0.0)	42	36	27	29	28	30	33	30	24	42
	EWS	30.9 (-1.2)	41	31	25	28	33	27	31	29	23	40

Table 3. Mean flip rate (mFR) on ImageNet-P, testing stability of predictions on (corrupted) videos. In line with Table 2, EWS improves consistently over all considered data augmentation schemes and nearly all corruption types. Similar to Table 2, Dropout did not improve over AutoAugment, AugMix or DeepAugment.

Results and Discussions. Table 1 shows that EWS is able to improve both clean and corrupted test errors on all three data augmentation schemes, *i.e.*, “standard”, AutoAugment and AugMix. Specifically, in terms of clean error, we are able to improve over AugMix by 0.79%, achieving an error of 3.56%. Furthermore, our method outperforms Dropout in all settings. As Dropout can be interpreted as randomly selecting channels in the preceding layers, it is a natural baseline to compare our EWS against. More critically, our method reduces the corrupted test error across all the settings. For example, with AugMix, EWS reduces the error by 2.77%, from 13.57% to 10.80%. The improvement is equally significant for AutoAugment and vanilla data augmentation (1.88% and 1.52%, respectively). We emphasize that the improvement gets more significant with more complex data augmentation. Overall, this highlights that EWS is entirely complementary to state-of-the-art data augmentation.

4.1.2 Results on ImageNet

Experimental Setup. Again, we adopt a ResNet-50 as the baseline model and, following [26], we use the learning rate warm-up for the first 5 epochs and train the model for 180 epochs in total. In addition to AutoAugment and Augmix, we consider DeepAugment [24] using the hyper-parameters proposed by the authors.

Results and Discussions. In Figure 4 (left), we first show that EWS consistently improves clean test error on top of all considered data augmentation schemes. In practice, we

reduce the error by at least 0.3% across all cases. When equipped with AugMix, our EWS yields the best error of 22.1% across all the considered settings. The improvement of EWS can be also observed throughout the whole training process, as illustrated for the standard data augmentation scheme in Figure 4 (right).

Table 2 and 3 highlight that the improvement obtained by EWS is even more significant on ImageNet-C and ImageNet-P. Specifically, on ImageNet-C, mean corruption error (mCE) reduces for all data augmentation schemes, including DeepAugment where mCE reduces from 60.4% to 58.9% (1.5% improvement). We also highlight that EWS improves results across most included corruption types. For DeepAugment, EWS only reduces performance on the included snow corruption. Regarding ImageNet-P, these observations are very much confirmed: mean flip rate (mFR) reduces from 32.1% to 30.9% (1.2% improvement) on top of DeepAugment and improvements are obtained across all corruptions except snow. Overall, these results indicate that improving the performance of subnets through EWS boosts clean and corrupted error across a range of state-of-the-art data augmentation schemes.

4.2. Improving Adversarial Robustness

Experimental Setup. We apply our EWS on top of three popular adversarial training variants to improve adversarial robustness on CIFAR-10: “standard” adversarial training (AT) [38], TRADES [69] and adversarial weight perturba-

Method		PreAct ResNet-18			WRN-28-10			WRN-34-10		
		Clean ↓	PGD-20 ↓	AA ↓	Clean ↓	PGD-20 ↓	AA ↓	Clean ↓	PGD-20 ↓	AA ↓
AT	Vanilla [38]	17.54	49.18	52.96 (-0.00)	14.89	45.17	47.81 (-0.00)	14.74	45.39	47.47 (-0.00)
	EWS	16.85	47.99	51.84 (-1.12)	14.57	44.24	47.17 (-0.64)	14.33	44.04	46.58 (-0.89)
TRADES	AWP [65]	19.59	46.01	51.43 (-0.00)	15.89	42.93	46.41 (-0.00)	14.17	41.89	45.96 (-0.00)
	AWP-EWS	19.25	44.98	50.48 (-0.95)	15.81	41.72	45.58 (-0.83)	14.21	41.07	45.29 (-0.67)
TRADES	Vanilla [69]	17.42	46.88	50.84 (-0.00)	15.50	44.11	47.40 (-0.00)	15.32	43.84	46.89 (-0.00)
	EWS	17.10	45.73	49.67 (-1.17)	15.09	43.45	46.72 (-0.68)	14.56	43.13	46.06 (-0.83)
TRADES	AWP [65]	18.27	45.36	49.62 (-0.00)	14.84	41.25	44.86 (-0.00)	15.55	40.85	43.90 (-0.00)
	AWP-EWS	16.67	44.20	48.58 (-1.04)	14.30	40.40	44.22 (-0.64)	14.13	40.05	43.17 (-0.73)

Table 4. Clean and robust test error, *i.e.*, on adversarial examples generated using PGD-20 or AutoAttack, for three different architectures: PreAct ResNet-18, WRN-28-10 and WRN-34-10. We consider ‘‘vanilla’’ AT as well as TRADES, see text, combined with AWP and/or the proposed EWS. We also report the improvement against AutoAttack in parentheses. Across all the settings, EWS reduces not only robust test error, *i.e.*, adversarial robustness, but also clean error.

tions (AWP) [65]. Following Section 3.4, this means we use the cross-entropy loss as ϕ in Eqn. (3) for AT and the KL divergence as ϕ for TRADES. We set $\gamma = 0$ for AT and, following [69], $\gamma = 1/6$ for TRADES. We consider PreAct ResNet-18 [23] as well as WRN-28-10 and WRN-34-10 [68] and employ early stopping [46]. For AWP, we follow the hyper-parameters of the original paper [65]. During training, we use projected gradient descent (PGD) with $p = \infty$ and $\epsilon = 8/255$ with 10 iterations. To evaluate the robustness on the test set, we report the robust error on PGD with 20 iterations and AutoAttack (AA) [9]. For EWS, we use the same hyper-parameters in Section 4.1.

Results and Discussions. In Table 4, combined with state-of-the-art adversarial training methods, our EWS improves adversarial robustness across all architectures. Moreover, the robustness-accuracy trade-off is improved [55,61]. For example, considering vanilla AT, EWS reduces clean test error of our PreAct ResNet-18 by 1.19% and robust test error on the standard AA benchmark by 1.12%. While the improvement gets slightly smaller for larger models, *i.e.*, WRN-28-10 and WRN-34-10, EWS improves both clean and robust test error consistently. On a WRN-34-10, the improvement in robust test error is still 0.89%. This also generalizes to TRADES, which generally improves adversarial robustness. Moreover, EWS is able to improve over TRADES with AWP which performs best in our experiments. Here, EWS reduces the robust test error from 43.90% to 43.17% (0.73% improvement). At the same time, EWS also reduces the clean error by 1.42%. This indicates that utilizing adversarial weight perturbations [65] on weak subnets instead of the overall network is more beneficial.

5. Ablation and Discussions

In the following, we present further ablation experiments and discussions. Specifically, in Section 5.1, we elaborate on the chosen hyper-parameters: We compare different search strategies to demonstrate the effectiveness of the proposed search algorithm. We also investigate the controller’s training interval K . Furthermore, we study the weight of the

Method	Clean Error ↓	Corruption Error ↓
Baseline	5.32	26.46
Random Search	4.49	25.81
L_1 -norm Selection	4.37	25.45
Subnet Search (Ours)	4.12	24.94

Table 5. Clean and corrupted test error on CIFAR-10 and CIFAR-10-C. We compare our search method with random search and a L_1 -norm based heuristic method, see text for details. While randomly selecting subnets to improve already reduces both clean and corrupted error, finding particularly weak subnets using the proposed search strategies obtains the lowest errors.

distillation loss λ and the width of the selected subnets ρ . Besides, EWS allows to analyze the vulnerability of individual blocks and layers, which we discuss in Section 5.2.

5.1. Search Strategies and Hyper-Parameters

We perform ablation studies on CIFAR-10 to choose search strategy and hyper-parameters for our EWS. For all the experiments, we train a ResNet-50 and adopt the same settings mentioned in Section 4.1.1.

Search strategies. In Table 5, we conduct an ablation study to investigate the effectiveness of our search method. We compare our method to two baselines: random search selects subnets entirely at random; and L_1 -norm selection chooses the channels/paths with lowest L_1 -norm of weights. For simplicity, we compare clean and corrupted test error on CIFAR-10(-C). Since the randomly sampled subnets may contain some weak components, we are able to reduce both the clean and corrupted error. Using L_1 -norm is a simple heuristic to find weaker subnets than random search. This can be seen by a slightly reduced clean and corrupted error. Nevertheless, the L_1 -norm may not be highly correlated with accuracy and the search results are often suboptimal. In contrast, our method yields the lowest clean and corrupted errors as the controller directly finds subnets with low accuracy.

Training cost. As detailed in Section 3.3 and Algorithm 1, we train the controller model every K epochs. Thus, we expect a trade-off between training cost and performance:

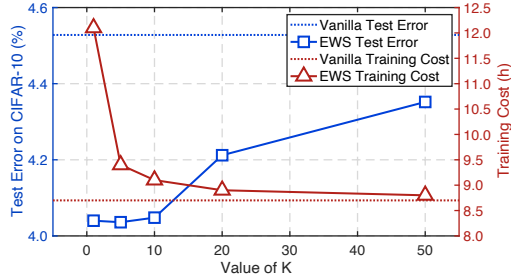


Figure 5. We plot (clean) test error on CIFAR-10 (blue) and training cost in hours (red) against the controller training interval K , see Algorithm 1. Clearly, increasing K reduces training cost significantly. At the same time, clean error reduces significantly for $K \leq 10$. These observations confirm our choice of $K = 10$.

a stronger controller model should improve performance, but needs to be updated more often (*i.e.*, lower K) which, however, increases the training cost. In Figure 5, we investigate the impact of K on clean test error (on CIFAR-10) by considering a set of values $\{1, 5, 10, 20, 50\}$. Gradually increasing K greatly reduces the training cost. Note that we obtain promising results for $K \leq 10$ but observe a significant increase of test error when $K > 10$. This justifies our choice of $K = 10$ in the experiments.

Weight of distillation loss. In Figure 6 (left), we change the value of λ in Eqn. (2). Note that $\lambda = 0$ corresponds to training *without* EWS. Larger λ , in contrast, increases the effect of EWS, *i.e.*, trying to enhance weak subnets more aggressively. Given a set of values $\lambda \in \{0, 0.001, 0.01, 0.1, 1, 10\}$, we gradually reduce clean test error up until $\lambda = 1$. Larger values will result in a small performance degradation. However, even $\lambda = 10$ still outperforms training without EWS. This generalizes across all considered data augmentation schemes, including AutoAugment and AugMix.

Subnet width. In Figure 6 (right), we investigate the impact of subnet width ρ on the performance improvement obtained using EWS. To this end, we consider a set of candidate widths $\rho \in \{0.1, 0.3, 0.5, 0.7, 0.9\}$. We suspect that very small subnets ($\rho=0.1$) cause the distillation loss $\mathcal{L}_{\text{KL}}(\alpha(x), M(x))$ to be very large, hampering the training process. When we increase ρ to 0.5 and 0.7, EWS yields significantly better results. For a larger $\rho \geq 0.9$, the distillation loss can be very small, performance drops again. Note that the distillation loss becomes 0 when $\rho = 1$ (*i.e.*, $\alpha = M$).

5.2. Vulnerability of Blocks and Layers

As mentioned in Section 3.1, we construct subnets by selecting a subset of paths and channels. This also allows us to investigate the vulnerability of each block. To this end, we construct subnets by randomly selecting a subset of paths/channels in a specific block, while keeping all other blocks unchanged. In Figure 7, we report test error on ImageNet when randomly sampling 100 subnets. From these results, by enhancing weak subnets during training through

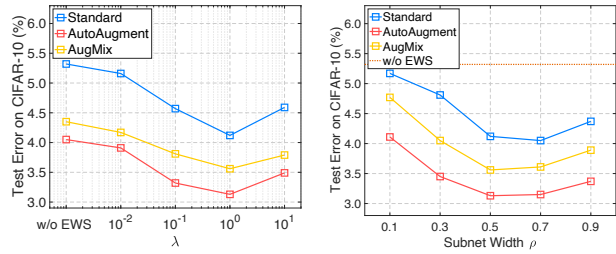


Figure 6. Clean test error on CIFAR-10 plotted against the weight of the distillation loss (left, see Algorithm 1) and the subnet width ρ (right). *Left:* Across all tested data augmentation schemes, including AutoAugment and AugMix, $\lambda = 1$ performs best. *Right:* Too small or too large subnets during training reduce the benefit of EWS. We found $\rho = 0.5$, *i.e.*, subnets representing roughly 50% of paths/channels, to perform best in most cases.

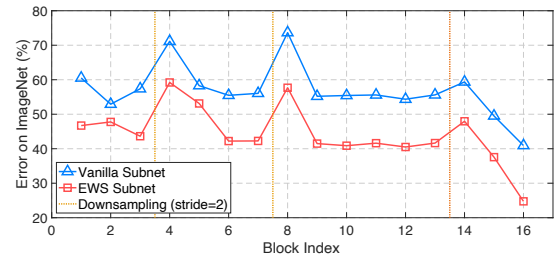


Figure 7. Test error on ImageNet when constructing subnets by randomly selecting 50% of paths/channels in a specific block while the remaining blocks are left unchanged. The results are averaged across 100 sampled subnets. The dotted line (orange) marks blocks with downsampling operation. Clearly, blocks *after* downsampling blocks are most vulnerable and the last two blocks are least vulnerable. In all cases, EWS reduces error on subnets significantly.

EWS, we can consistently lower test error (across all blocks) compared to standard training. Moreover, the blocks/layers behind the downsampling operation (highlighted in dotted lines) tend to be more vulnerable than the other layers.

6. Conclusion

In this paper, we focused on improving model robustness and investigated the behaviors of subnets inside a full model. We observe that weak subnet performance is correlated with lacking robustness against corruptions and adversarial attacks of the full network. Regarding this issue, we have developed a novel robust training method which explicitly identifies and *enhances weak subnets (EWS)*. Specifically, we first develop a search algorithm to find weak subnets and then strengthen them via knowledge distillation from the full model. Experiments show that, combined with diverse data augmentation schemes and adversarial training approaches, EWS significantly improves the corruption and adversarial robustness on several benchmark datasets.

References

- [1] Naveed Akhtar and Ajmal Mian. Threat of adversarial attacks on deep learning in computer vision: A survey. *IEEE Access*, 6:14410–14430, 2018. [2](#)
- [2] Marco Barreno, Blaine Nelson, Russell Sears, Anthony D. Joseph, and J. D. Tygar. Can machine learning be secure? In *Proc. of the ACM on Asia Conference on Computer and Communications Security (AsiaCCS)*, 2006. [2](#)
- [3] Philipp Benz, Chaoning Zhang, Adil Karjauv, and In So Kweon. Revisiting batch normalization for improving corruption robustness. In *Proc. of the IEEE Winter Conference on Applications of Computer Vision (WACV)*, pages 494–503, 2021. [2](#)
- [4] Battista Biggio and Fabio Roli. Wild patterns: Ten years after the rise of adversarial machine learning. *Pattern Recognition*, 84:317–331, 2018. [2](#)
- [5] Han Cai, Ligeng Zhu, and Song Han. ProxylessNAS: Direct neural architecture search on target task and hardware. In *Proc. of the International Conference on Learning Representations (ICLR)*, 2019. [2](#)
- [6] Dan A. Calian, Florian Stimberg, Olivia Wiles, Sylvestre-Alvise Rebuffi, András György, Timothy A. Mann, and Sven Gowal. Defending against image corruptions through adversarial augmentations. *arXiv.org*, abs/2104.01086, 2021. [2](#)
- [7] Yair Carmon, Aditi Raghunathan, Ludwig Schmidt, Percy Liang, and John Duchi. Unlabeled data improves adversarial robustness. In *Advances in Neural Information Processing Systems (NIPS)*, 2019. [2](#)
- [8] Yaofu Chen, Yong Guo, Qi Chen, Minli Li, Wei Zeng, Yaowei Wang, and Mingkui Tan. Contrastive neural architecture search with neural architecture comparators. In *Proc. of the IEEE Conference on Computer Vision and Pattern Recognition (CVPR)*, pages 9502–9511, 2021. [2](#)
- [9] Francesco Croce and Matthias Hein. Reliable evaluation of adversarial robustness with an ensemble of diverse parameter-free attacks. In *Proc. of the International Conference on Machine Learning (ICML)*, 2020. [7](#)
- [10] Ekin D Cubuk, Barret Zoph, Dandelion Mane, Vijay Vasudevan, and Quoc V Le. Autoaugment: Learning augmentation policies from data. In *Proc. of the IEEE Conference on Computer Vision and Pattern Recognition (CVPR)*, 2019. [1](#), [2](#), [4](#), [5](#), [6](#), [14](#), [15](#)
- [11] Jia Deng, Wei Dong, Richard Socher, Li-Jia Li, Kai Li, and Li Fei-Fei. Imagenet: A large-scale hierarchical image database. In *Proc. of the IEEE Conference on Computer Vision and Pattern Recognition (CVPR)*, pages 248–255, 2009. [5](#)
- [12] Jonathan Frankle and Michael Carbin. The lottery ticket hypothesis: Training pruned neural networks. *arXiv.org*, abs/1803.03635, 2018. [1](#)
- [13] Robert Geirhos, Patricia Rubisch, Claudio Michaelis, Matthias Bethge, Felix A Wichmann, and Wieland Brendel. Imagenet-trained cnns are biased towards texture; increasing shape bias improves accuracy and robustness. *Proc. of the International Conference on Learning Representations (ICLR)*, 2019. [2](#)
- [14] Ian J Goodfellow, Jonathon Shlens, and Christian Szegedy. Explaining and harnessing adversarial examples. In *Proc. of the International Conference on Learning Representations (ICLR)*, 2015. [1](#), [2](#)
- [15] Jianping Gou, Baosheng Yu, Stephen J Maybank, and Dacheng Tao. Knowledge distillation: A survey. 129(6):1789–1819, 2021. [2](#)
- [16] Sven Gowal, Chongli Qin, Jonathan Uesato, Timothy A. Mann, and Pushmeet Kohli. Uncovering the limits of adversarial training against norm-bounded adversarial examples. *arXiv.org*, abs/2010.03593, 2020. [1](#)
- [17] Sven Gowal, Sylvestre-Alvise Rebuffi, Olivia Wiles, Florian Stimberg, Dan Andrei Calian, and Timothy Mann. Improving robustness using generated data. *arXiv preprint arXiv:2110.09468*, 2021. [2](#)
- [18] Alex Graves. Long short-term memory. In *Supervised sequence labelling with recurrent neural networks*, pages 37–45. Springer, 2012. [4](#)
- [19] Yong Guo, Yaofu Chen, Yin Zheng, Peilin Zhao, Jian Chen, Junzhou Huang, and Mingkui Tan. Breaking the curse of space explosion: Towards efficient nas with curriculum search. In *Proc. of the International Conference on Machine Learning (ICML)*, pages 3822–3831. PMLR, 2020. [2](#), [4](#), [12](#), [13](#)
- [20] Yong Guo, Yin Zheng, Mingkui Tan, Qi Chen, Jian Chen, Peilin Zhao, and Junzhou Huang. Nat: Neural architecture transformer for accurate and compact architectures. In *NeurIPS*, pages 735–747, 2019. [4](#)
- [21] Yong Guo, Yin Zheng, Mingkui Tan, Qi Chen, Zhipeng Li, Jian Chen, Peilin Zhao, and Junzhou Huang. Towards accurate and compact architectures via neural architecture transformer. *IEEE Trans. on Pattern Analysis and Machine Intelligence (PAMI)*, 2021. [2](#)
- [22] Kaiming He, Xiangyu Zhang, Shaoqing Ren, and Jian Sun. Deep residual learning for image recognition. In *Proc. of the IEEE Conference on Computer Vision and Pattern Recognition (CVPR)*, pages 770–778, 2016. [1](#), [2](#), [3](#)
- [23] Kaiming He, Xiangyu Zhang, Shaoqing Ren, and Jian Sun. Identity mappings in deep residual networks. In *Proc. of the European Conference on Computer Vision (ECCV)*, pages 630–645. Springer, 2016. [7](#), [15](#)
- [24] Dan Hendrycks, Steven Basart, Norman Mu, Saurav Kadavath, Frank Wang, Evan Dorundo, Rahul Desai, Tyler Zhu, Samyak Parajuli, Mike Guo, et al. The many faces of robustness: A critical analysis of out-of-distribution generalization. In *Proc. of the IEEE International Conference on Computer Vision (ICCV)*, pages 8340–8349, 2021. [1](#), [2](#), [4](#), [5](#), [6](#), [14](#), [15](#)
- [25] Dan Hendrycks and Thomas G. Dietterich. Benchmarking neural network robustness to common corruptions and perturbations. In *Proc. of the International Conference on Learning Representations (ICLR)*, 2019. [1](#), [2](#)
- [26] Dan Hendrycks, Norman Mu, Ekin D Cubuk, Barret Zoph, Justin Gilmer, and Balaji Lakshminarayanan. Augmix: A simple data processing method to improve robustness and uncertainty. In *Proc. of the International Conference on Learning Representations (ICLR)*, 2020. [1](#), [2](#), [4](#), [5](#), [6](#), [14](#), [15](#)
- [27] Geoffrey Hinton, Oriol Vinyals, and Jeff Dean. Distilling the knowledge in a neural network. In *NeurIPS Deep Learning and Representation Learning Workshop*, 2014. [2](#)

[28] Klim Kireev, Maksym Andriushchenko, and Nicolas Flammarion. On the effectiveness of adversarial training against common corruptions. *arXiv.org*, abs/2103.02325, 2021. 2

[29] Alex Krizhevsky and Geoffrey Hinton. Learning multiple layers of features from tiny images, 2009. 5

[30] Alex Krizhevsky, Ilya Sutskever, and Geoffrey E Hinton. Imagenet classification with deep convolutional neural networks. In *Advances in Neural Information Processing Systems (NIPS)*, pages 1097–1105, 2012. 1

[31] Alex Lamb, Vikas Verma, Juho Kannala, and Yoshua Bengio. Interpolated adversarial training: Achieving robust neural networks without sacrificing too much accuracy. In *Proceedings of the 12th ACM Workshop on Artificial Intelligence and Security*, pages 95–103, 2019. 2

[32] Yann LeCun, Bernhard Boser, John S Denker, Donnie Henderson, Richard E Howard, Wayne Hubbard, and Lawrence D Jackel. Backpropagation applied to handwritten zip code recognition. *Neural Computation*, 1(4):541–551, 1989. 1

[33] Chen-Yu Lee, Saining Xie, Patrick Gallagher, Zhengyou Zhang, and Zhuowen Tu. Deeply-supervised nets. In *AISTATS*, 2015. 1

[34] Bai Li, Shiqi Wang, Yunhan Jia, Yantao Lu, Zhenyu Zhong, Lawrence Carin, and Suman Jana. Towards practical lottery ticket hypothesis for adversarial training. *arXiv.org*, abs/2003.05733, 2020. 1, 2

[35] Chenxi Liu, Liang-Chieh Chen, Florian Schroff, Hartwig Adam, Wei Hua, Alan L Yuille, and Li Fei-Fei. Auto-deeplab: Hierarchical neural architecture search for semantic image segmentation. In *Proc. of the IEEE Conference on Computer Vision and Pattern Recognition (CVPR)*, pages 82–92, 2019. 2

[36] Hanxiao Liu, Karen Simonyan, and Yiming Yang. Darts: Differentiable architecture search. In *Proc. of the International Conference on Learning Representations (ICLR)*, 2019. 2, 3

[37] Divyam Madaan, Jinwoo Shin, and Sung Ju Hwang. Learning to generate noise for robustness against multiple perturbations. *arXiv.org*, abs/2006.12135, 2020. 2

[38] Aleksander Madry, Aleksandar Makelov, Ludwig Schmidt, Dimitris Tsipras, and Adrian Vladu. Towards deep learning models resistant to adversarial attacks. In *Proc. of the International Conference on Learning Representations (ICLR)*, 2018. 1, 2, 4, 5, 6, 7, 15

[39] Pratyush Maini, Eric Wong, and Zico Kolter. Adversarial robustness against the union of multiple perturbation models. In *Proc. of the International Conference on Machine Learning (ICML)*, pages 6640–6650. PMLR, 2020. 2

[40] Xiaofeng Mao, Gege Qi, Yuefeng Chen, Xiaodan Li, Ranjie Duan, Shaokai Ye, Yuan He, and Hui Xue. Towards robust vision transformer. *arXiv.org*, abs/2105.07926, 2021. 2

[41] Seyed-Mohsen Moosavi-Dezfooli, Alhussein Fawzi, Omar Fawzi, and Pascal Frossard. Universal adversarial perturbations. In *Proc. of the IEEE Conference on Computer Vision and Pattern Recognition (CVPR)*, pages 1765–1773, 2017. 2

[42] Zachary Nado, Shreyas Padhy, D. Sculley, Alexander D’Amour, Balaji Lakshminarayanan, and Jasper Snoek. Evaluating prediction-time batch normalization for robustness under covariate shift. *arXiv.org*, abs/2006.10963, 2020. 2

[43] Tianyu Pang, Xian Yang, Yinpeng Dong, Hang Su, and Jun Zhu. Bag of tricks for adversarial training. *Proc. of the International Conference on Learning Representations (ICLR)*, 2021. 1

[44] Hieu Pham, Melody Y Guan, Barret Zoph, Quoc V Le, and Jeff Dean. Efficient neural architecture search via parameter sharing. In *Proc. of the International Conference on Machine Learning (ICML)*, pages 4092–4101, 2018. 3, 4, 12, 13

[45] Sylvestre-Alvise Rebuffi, Sven Gowal, Dan A Calian, Florian Stimberg, Olivia Wiles, and Timothy Mann. Fixing data augmentation to improve adversarial robustness. *arXiv preprint arXiv:2103.01946*, 2021. 2

[46] Leslie Rice, Eric Wong, and J. Zico Kolter. Overfitting in adversarially robust deep learning. In *Proc. of the International Conference on Machine Learning (ICML)*, 2020. 7

[47] E. Rusak, Lukas Schott, R. S. Zimmermann, Julian Bitterwolf, O. Bringmann, M. Bethge, and W. Brendel. A simple way to make neural networks robust against diverse image corruptions. In *Proc. of the European Conference on Computer Vision (ECCV)*, 2020. 2

[48] Olga Russakovsky, Jia Deng, Hao Su, Jonathan Krause, Sanjeev Satheesh, Sean Ma, Zhiheng Huang, Andrej Karpathy, Aditya Khosla, Michael Bernstein, et al. Imagenet large scale visual recognition challenge. *IJCV*, 115(3):211–252, 2015. 1

[49] Tonmoy Saikia, Cordelia Schmid, and Thomas Brox. Improving robustness against common corruptions with frequency biased models. *arXiv.org*, abs/2103.16241, 2021. 2

[50] Hadi Salman, Andrew Ilyas, Logan Engstrom, Ashish Kapoor, and Aleksander Madry. Do adversarially robust imagenet models transfer better? *Advances in Neural Information Processing Systems (NIPS)*, 2020. 2

[51] Steffen Schneider, Evgenia Rusak, Luisa Eck, Oliver Bringmann, Wieland Brendel, and Matthias Bethge. Improving robustness against common corruptions by covariate shift adaptation. *Advances in Neural Information Processing Systems (NIPS)*, 33, 2020. 2

[52] Vikash Sehwag, Shiqi Wang, Prateek Mittal, and Suman Jana. Hydra: Pruning adversarially robust neural networks. *Advances in Neural Information Processing Systems (NIPS)*, 33, 2020. 1, 2

[53] Samuel Henrique Silva and Peyman Najafirad. Opportunities and challenges in deep learning adversarial robustness: A survey. *arXiv.org*, abs/2007.00753, 2020. 2

[54] Nitish Srivastava, Geoffrey E Hinton, Alex Krizhevsky, Ilya Sutskever, and Ruslan Salakhutdinov. Dropout: a simple way to prevent neural networks from overfitting. *JMLR*, 15(1):1929–1958, 2014. 5, 14

[55] David Stutz, Matthias Hein, and Bernt Schiele. Disentangling adversarial robustness and generalization. *Proc. of the IEEE Conference on Computer Vision and Pattern Recognition (CVPR)*, 2019. 5, 7

[56] David Stutz, Matthias Hein, and Bernt Schiele. Confidence-calibrated adversarial training: Generalizing to unseen attacks. In *Proc. of the International Conference on Machine Learning (ICML)*, 2020. 2

[57] David Stutz, Matthias Hein, and Bernt Schiele. Relating adversarially robust generalization to flat minima. In *Proc.*

of the IEEE International Conference on Computer Vision (ICCV), 2021. 2

[58] Siqi Sun, Yu Cheng, Zhe Gan, and Jingjing Liu. Patient knowledge distillation for bert model compression. *Proc. of the Conference on Empirical Methods in Natural Language Processing*, 2019. 2

[59] Christian Szegedy, Wojciech Zaremba, Ilya Sutskever, Joan Bruna, Dumitru Erhan, Ian Goodfellow, and Rob Fergus. Intriguing properties of neural networks. *Proc. of the International Conference on Learning Representations (ICLR)*, 2014. 1, 2

[60] Florian Tramèr and Dan Boneh. Adversarial training and robustness for multiple perturbations. *arXiv.org*, abs/1904.13000, 2019. 2

[61] Dimitris Tsipras, Shibani Santurkar, Logan Engstrom, Alexander Turner, and Aleksander Madry. Robustness may be at odds with accuracy. In *Proc. of the International Conference on Learning Representations (ICLR)*, 2019. 7

[62] Jonathan Uesato, Jean-Baptiste Alayrac, Po-Sen Huang, Robert Stanforth, Alhussein Fawzi, and Pushmeet Kohli. Are labels required for improving adversarial robustness? *Advances in Neural Information Processing Systems (NIPS)*, 2019. 2

[63] Ning Wang, Yang Gao, Hao Chen, Peng Wang, Zhi Tian, Chunhua Shen, and Yanning Zhang. Nas-fcos: Fast neural architecture search for object detection. In *Proc. of the IEEE Conference on Computer Vision and Pattern Recognition (CVPR)*, pages 11943–11951, 2020. 2

[64] Yisen Wang, Difan Zou, Jinfeng Yi, James Bailey, Xingjun Ma, and Quanquan Gu. Improving adversarial robustness requires revisiting misclassified examples. In *Proc. of the International Conference on Learning Representations (ICLR)*, 2020. 2

[65] Dongxian Wu, Shu-Tao Xia, and Yisen Wang. Adversarial weight perturbation helps robust generalization. *Advances in Neural Information Processing Systems (NIPS)*, 2020. 2, 4, 5, 7, 15

[66] Han Xu, Yao Ma, Haochen Liu, Debayan Deb, Hui Liu, Jiliang Tang, and Anil K. Jain. Adversarial attacks and defenses in images, graphs and text: A review. *International Journal of Automation and Computing (IJAC)*, 2020. 2

[67] Xiaoyong Yuan, Pan He, Qile Zhu, Rajendra Rana Bhat, and Xiaolin Li. Adversarial examples: Attacks and defenses for deep learning. *IEEE Trans. on Neural Networks and Learning Systems (TNNLS)*, 2017. 2

[68] Sergey Zagoruyko and Nikos Komodakis. Wide residual networks. In *BMVC*, 2016. 7, 15

[69] Hongyang Zhang, Yaodong Yu, Jiantao Jiao, Eric Xing, Laurent El Ghaoui, and Michael Jordan. Theoretically principled trade-off between robustness and accuracy. In *Proc. of the International Conference on Machine Learning (ICML)*, pages 7472–7482. PMLR, 2019. 2, 4, 5, 6, 7, 15

[70] Bojia Zi, Shihao Zhao, Xingjun Ma, and Yu-Gang Jiang. Revisiting adversarial robustness distillation: Robust soft labels make student better. *Proc. of the IEEE Conference on Computer Vision and Pattern Recognition (CVPR)*, 2021. 2, 14

[71] Barret Zoph and Quoc V Le. Neural architecture search with reinforcement learning. In *Proc. of the International Conference on Learning Representations (ICLR)*, 2017. 2

Supplementary Materials for “Improving Corruption and Adversarial Robustness by Enhancing Weak Subnets”

In the main paper, we developed a robust training method which explicitly identifies and **enhances weak subnets (EWS)** during training to improve the overall robustness. Specifically, we develop a search algorithm to find particularly weak subnets and propose to explicitly strengthen these subnets via knowledge distillation from the full network. In the experiments, we have shown that our EWS improves the corruption and adversarial robustness when applied on top of diverse data augmentation schemes and popular adversarial training methods, respectively. In the supplementary, we provide additional discussions, more implementation details, and complementary experimental results of our EWS.

We organize the supplementary as follows:

- In Section A, we provide a concrete example to show how the controller model generates subnets.
- In Section B, we investigate the impact of the size of training data for search.
- In Section C, we empirically compare different losses for enhancing subnets in our EWS.
- In Section D, we provide more implementation details and results for improving corruption robustness.
- In Section E, we provide more implementation details and results for improving adversarial robustness.

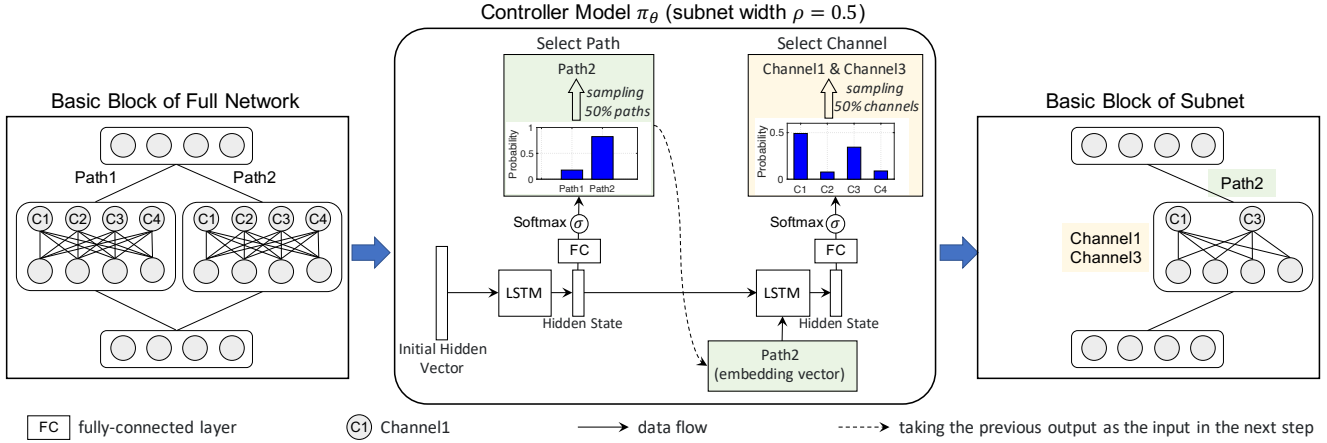


Figure A. A concrete example of generating subnets using the controller model for a block with 2 paths, each of which has 4 channels. When constructing subnets, we consider the subset width $\rho = 0.5$, *i.e.*, selecting one path and two channels. As illustrated, the LSTM based controller model takes an initial hidden state as input to predict the hidden vector for path selection. Then, we exploit a full-connected (FC) layer followed by a Softmax function to produce the probability distribution of two candidate paths. After that, we perform sampling on the distribution to select the weakest path, *i.e.*, “Path2”. As for channel selection, similarly, we take the embedding of the selected path (*i.e.*, “Path2”) and previous hidden state as inputs. We also use a Softmax classifier to predict the probability distribution of candidate channels. Considering the subnet width $\rho = 0.5$, we sample two channels without replacement from the distribution, *i.e.*, Channel1 and Channel3.

A. Generating Candidate Subnets using the Controller Model

As mentioned in Section 3.2, following [19, 44], the controller model takes an initial hidden vector as input and then sequentially selects candidate paths/channels starting from the first block/layer to the last one. Essentially, the subnet generation process is a Markov Decision Process (MDP). In other words, we sequentially make decisions and each decision relies on

a previous one. To better illustrate this, we show a concrete example of subnet generation using our controller model. In Figure A, we take a block with 2 paths, each of which has 4 channels, for example. As illustrated in the figure, the controller model first predicts the hidden vector as output and then exploits a softmax classifier (*i.e.*, a single full-connected layer) to obtain the probability distribution of candidate paths. Based on the predicted probability distribution, we perform sampling without replacement to determine the weak paths, *e.g.*, “Path2” in Figure A. After that, in the next step, we then take the selected path (represented by an embedding vector method, see details below) and the previous hidden state as the inputs of LSTM to select weak channels (*e.g.*, Channel1 and Channel3). Finally, we combine all the selected paths and channels to obtain a whole subnet. Note that different blocks/layers may have different numbers of paths/channels. Regarding this issue, we initialize the number of neurons in the classifier with the maximum number of paths/channels across all the blocks/layers. In this way, given a block/layer with C candidate paths/channels, we only focus on the first C output logits when applying the softmax transformation and subsequently performing sampling.

Representation of Candidate Paths and Channels. To represent different paths and channels, we follow [19, 44] and build a learnable embedding vector for each of them. In this paper, we use a 100-dimensional vector to represent each path or channel in the full network. It is worth noting that, since we sample paths/channels without replacement from the predicted probability distribution, our method allows to simultaneously select multiple components (*e.g.*, selecting two channels in Figure A). To feed them as input in the next decision step, we compute the average embedding over all the selected components. For example, for the considered block in Figure A, we compute the average embedding over both Channel1 and Channel3 as the input for the decision of the next block.

B. Impact of the Size of Training Data for Search

As we discussed in Section 3.2, we construct a subset $\mathcal{D}_s \subset \mathcal{D}$ as a proxy dataset to accelerate the search process, where \mathcal{D} denotes the training dataset. Here, we investigate the impact of the subset size on both the performance and training cost of our EWS. In this experiment, we construct the subset using $\{1\%, 5\%, 10\%, 30\%, 50\%\}$ data of CIFAR-10. As shown in Figure B, the training cost gradually increases with the increase of the subset size. Here, the training time is measured on two NVIDIA Quadro RTX 8000 GPUs when training a ResNet-50 model for 400 epochs. Nevertheless, as for the test error, we observe a significant performance improvement when we increase the subset size from 1% to 10%. When we further increase the subset size (*e.g.*, 30% and 50%), we observe very small performance improvement in practice. Based on these results, we choose to construct the training subset for search using 10% data to balance training performance and training cost.

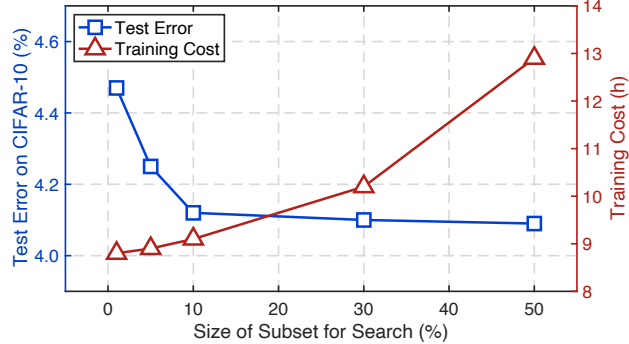


Figure B. We plot (clean) test error on CIFAR-10 (blue) and training cost in hours (red) against the size of training subset for search. We measure the total time of training a ResNet-50 model for 400 epochs based on two NVIDIA Quadro RTX 8000 GPUs. In general, the larger training subset we use, the higher training cost we obtain. As for the test error, we significantly reduce the error rate when we increase the subset size from 0% to 10% but yield similar results with the size larger than 10%. These results verify that constructing the training subset using 10% data to perform subnet search is a good choice for our EWS.

C. Comparison of Different Losses for Enhancing Subnets

In our EWS method, we exploit a Kullback-Leibler (KL) divergence loss $\mathcal{L}_{\text{KL}}(\alpha(x), M(x))$ to enhance weak subnets. To achieve this goal, we can also consider other forms of loss function. For example, we may directly minimize the cross-entropy (CE) loss of the subnet, *i.e.*, $\mathcal{L}_{\text{CE}}(\alpha(x), y)$. Here, we empirically compare these two losses on CIFAR-10 dataset. As shown in Table A, since both CE and KL losses enhance weak subnets, they yield better results than the vanilla model trained without

EWS. These results verify our idea of enhancing weak subnets. More critically, the KL loss outperforms the CE loss in terms of both clean error and corruption error. As argued in [70], this might be because the KL loss treats the output of the full network $M(x)$ as a kind of soft label, making optimization easier. Thus, we propose to use the KL loss to enhance weak subnets inside the full model.

Table A. Comparison of different forms of the distillation loss in terms of clean and corrupted test error on CIFAR10(-C). We compare the Kullback-Leibler (KL) divergence loss and cross-entropy (CE) loss. Clearly, the KL loss outperforms the CE loss in terms of both clean error and corruption error.

Loss for Enhancing Subnets	Clean Error (%)	Corruption Error (%)
Vanilla (w/o EWS)	5.32	26.46
$\mathcal{L}_{\text{CE}}(\alpha(x), y)$	4.73	25.81
$\mathcal{L}_{\text{KL}}(\alpha(x), M(x))$	4.12	24.94

D. More Details and Results of Improving Corruption Robustness

In the paper, we have conducted extensive experiments to show the effectiveness of EWS in improving corruption robustness. Specifically, we train deep models using EWS, equipped with diverse data augmentation schemes, on both CIFAR-10 and ImageNet data sets. Here, we provide more details of the experimental setup as well as more results.

Detailed Experimental Settings. We consider two benchmark data sets, namely CIFAR-10 and ImageNet. For the experiments on CIFAR-10, we train a ResNet-50 with 400 training epochs and use Nesterov momentum for optimization. We compare our EWS with the vanilla training method and Dropout [54]. By default, we use random cropping and horizontal flipping as data augmentation (we call it “standard” setting for convenience). Moreover, we also apply our EWS on top of state-of-the-art augmentation schemes, including AutoAugment [10] and AugMix [26]. When we apply our EWS on top of AugMix, we set the augmentation severity to 5 and exploit JSD loss during training. We set the initial learning rate to 0.1 and decrease it to 0.01 and 0.001 at the 1/3 and 2/3 of the total training process. For the hyper-parameters of EWS, we set $\lambda = 1$ and construct the training subset for search using 10% data. When training the controller model, we use policy gradient based on a mini-batch of 8 sampled subnets. As for the experiments on ImageNet, following [26], we train a ResNet-50 model for 180 epochs, with 5 epochs for warmup. In addition to AutoAugment and Augmix, we consider DeepAugment [24] using the hyper-parameters proposed by the authors. We adopt the same learning rate decay strategy as the experiments on CIFAR-10. As for EWS, we observe $\lambda = 0.7$ yields slightly better results than $\lambda = 1$ on ImageNet and use it in our experiments. We keep all the other hyper-parameters the same as those on CIFAR-10.

Table B. Mean corruption error (mCE) on ImageNet-C for the vanilla data augmentation scheme, AutoAugment, AugMix and DeepAugment. In all settings, EWS further reduces mCE. We also show mCE for all corruptions individually. For example, EWS improves over DeepAugment for all corruptions except snow.

Method		mCE ↓	Noise			Blur				Weather				Digital			
			Gauss.	Shot	Impulse	Defocus	Glass	Motion	Zoom	Snow	Frost	Fog	Bright	Contrast	Elastic	Pixel	JPEG
Standard	Vanilla	76.5	80	82	83	75	89	78	80	78	75	66	57	71	85	77	77
	Dropout	76.5	77	79	80	78	90	79	87	77	77	67	58	70	84	75	76
	EWS	75.1	75	76	77	73	87	77	79	80	73	65	58	73	83	74	75
AutoAugment [10]	Vanilla	72.7	69	68	72	77	83	80	81	79	75	64	56	70	88	57	71
	Dropout	73.5	72	70	71	78	85	82	80	81	76	66	56	71	90	56	72
	EWS	71.7	67	68	71	78	82	78	79	78	73	64	55	69	86	56	72
AugMix [26]	Vanilla	68.4	65	66	67	70	80	66	66	75	72	67	58	58	79	69	69
	Dropout	69.8	67	65	68	73	82	69	67	74	75	68	59	64	81	67	72
	EWS	67.5	64	63	63	70	81	65	66	72	70	64	57	63	79	64	70
DeepAugment [24]	Vanilla	60.4	49	50	47	59	73	65	76	64	60	58	51	61	76	48	67
	Dropout	61.0	50	51	48	61	74	65	72	65	63	59	54	62	76	49	67
	EWS	58.9	48	47	45	58	71	63	73	65	59	56	50	60	74	47	66

More Comparison Results. As mentioned in Tables 2 and 3, we omit the results of Dropout on top of AutoAugment, AugMix, and DeepAugment. In the supplementary, we provide the full results of these tables. As shown in Tables B and C, our EWS consistently outperforms Dropout across different augmentation schemes. The main reasons lie in the differences between our EWS and Dropout. *First*, they have different strategies of selecting subnets. Dropout entirely drops connections at random to select subnets. In contrast, EWS exploits the controller model to select weak subnets which may contribute to

Table C. Mean flip rate (mFR) on ImageNet-P, testing stability of predictions on (corrupted) videos. In line with Table 2, EWS improves consistently over all considered data augmentation schemes and nearly all corruption types.

Method		mFR ↓	Noise		Blur		Weather		Digital			
			Gaussian	Shot	Motion	Zoom	Snow	Bright	Translate	Rotate	Tilt	Scale
Standard	Vanilla	58.0	59	58	64	72	63	62	44	52	57	48
	Dropout	57.8	62	59	65	52	48	58	63	57	44	72
	EWS	56.1	62	55	62	49	45	52	64	52	42	71
AutoAugment [10]	Vanilla	51.7	50	45	57	68	63	53	40	44	50	46
	Dropout	53.3	53	49	54	67	67	55	44	48	51	47
	EWS	50.4	48	44	53	70	62	52	36	45	49	45
AugMix [26]	Vanilla	37.4	46	41	30	47	38	46	25	32	35	33
	Dropout	39.1	49	43	35	45	35	49	33	37	31	34
	EWS	36.6	45	39	31	42	33	43	39	35	27	32
DeepAugment [24]	Vanilla	32.1	42	36	27	29	28	30	33	30	24	42
	Dropout	39.1	49	43	35	45	35	49	33	37	31	34
	EWS	30.9	41	31	25	28	33	27	31	29	23	40

the poor robustness of the full network. *Second*, Dropout directly minimizes the cross-entropy loss w.r.t. the selected subnet. Unlike Dropout, our EWS enhances the subnet while training the full network. The improved performance over Dropout, in Tables B and C, verifies our idea of enhancing weak subnets.

E. More Details and Results of Improving Adversarial Robustness

To show the effectiveness in improving adversarial robustness, we have applied our EWS on top of popular adversarial training methods in the paper. In the supplementary, we provide more detailed experimental settings and more results.

Detailed Experimental Settings. We apply our EWS on top of three popular adversarial training variants on CIFAR-10, including AT [38], TRADES [69] and AWP [65]. Note that AWP is often applied to existing training approaches to further boost the performance. Here, we seek to highlight the improved adversarial robustness over both the vanilla AT and TRADES, as well as their AWP variants. For the experiments based on AT, we use the cross-entropy loss as ϕ in Eqn. (4) and set $\gamma = 0$. As for TRADES, we use the KL loss as ϕ and set $\gamma = 1/6$. We consider three deep models, namely PreAct ResNet-18 [23], WideResNets28/34 with the width factor of 10 [68]. During training, we employ early stopping and train the models for 200 epochs. We adopt the SGD optimizer using a batch size of 128, a step-wise learning rate decay set initially at 0.1 and divided by 10 at epochs 100 and 150, and weight decay 5×10^{-4} . Here, we use projected gradient descent (PGD) with $p = \infty$ and $\epsilon = 8/255$ with 10 iterations. For EWS, we set $\lambda = 1$ and use 10% data to construct the training subset for search.

More Comparison Results. In the paper, we have shown the improvement obtained by EWS on top of AT and TRADES in Table 4. Here, we further compare the convergence curves in Figure C. Clearly, for both AT and TRADES, no matter with or without AWP, our EWS (blue and red lines) consistently yields an obvious performance improvement in terms of robust accuracy against PGD-20. These results demonstrate the effectiveness of our EWS in improving adversarial robustness.

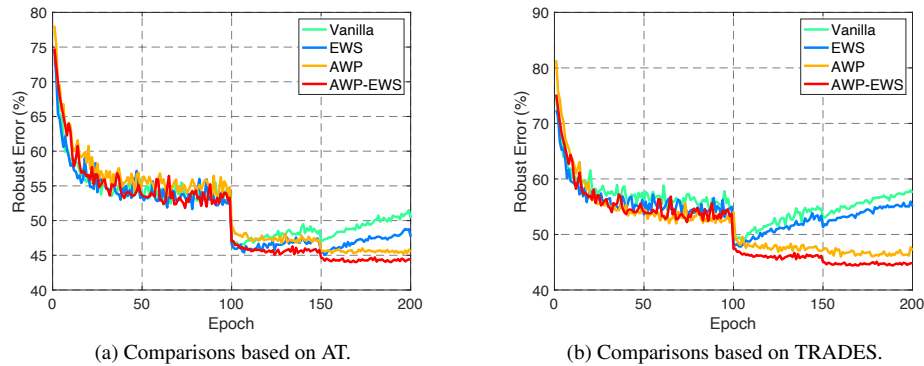


Figure C. Comparisons of convergence curves in terms of adversarial robust error on CIFAR-10. *Left*: Training curves obtained with and without EWS based on AT. *Right*: Training curves obtained with and without EWS based on TRADES. Clearly, our EWS consistently improves adversarial robustness over both the vanilla AT and TRADES as well as their AWP variants.